Available online at www.sciencedirect.com
SCIENCE DIRECT®
Bioorganic & Medicinal Chemistry 13 (2005) 6404–6413
Bioorganic & Medicinal Chemistry

Homology modelling and active-site-mutagenesis study of the catalytic domain of the pneumococcal phosphorylcholine esterase

Nuria Eugenia Campillo,[a,*,†] Juan Antonio Páez,[a,†] Laura Lagartera[b] and Ana Gonzalez[c]

[a]*Instituto de Química Médica (CSIC), Juan de la Cierva, N 28006-3, Madrid, Spain*
[b]*Dpto de Quimica-Física de Macromoléculas Biológicas, Instituto de Química Física Rocasolano (CSIC), Serrano 119, Madrid 28006, Spain*
[c]*Departamento de Microbiología Molecular, Centro de Investigaciones Biológicas (CSIC), Ramiro de Maeztu 9, Madrid 28040, Spain*

Received 2 February 2005; revised 28 June 2005; accepted 29 June 2005
Available online 19 August 2005

Abstract—*Streptococcus pneumoniae* is among the major human pathogens. Several interactions of this bacterium with its host appear to have been mediated by bacterial cell wall components. Specifically, phosphorylcholine residues covalently attached to teichoic and lipoteichoic acids serve as anchors for many surface-located proteins (choline-binding proteins CBPs), including cell-adhesion and virulence factors, and are also recognized by host response components through choline-binding receptors. In this study, we have performed modelling of the catalytic domain of pneumococcal phosphorylcholine esterase (Pce), a modular enzyme that is capable of removing phosphorycholine residues from teichoic and lipoteichoic acids, remodelling their distribution on the bacterial envelope. We wish to contribute to the structural knowledge of Pce. In this pursuit, 3D models of Pce have been established by homology modelling, using the X-ray structure of enzymes from the α/β metallo-lactamase family fold as templates. Theoretical models of pneumococcal phosphorylcholine esterase (Pce) catalytic modules obtained by homology modelling, and corresponding docking studies employed to find out the residues involved in the binding of Zn ions, are discussed according to mutational studies and ab initio calculations. The presence of a binuclear Zn cluster in the catalytic domain of Pce and a likely coordination model are proposed.

1. Introduction

Streptococcus pneumoniae is among the most frequent gram-positive pathogens. Pneumococcus can infect upper respiratory tracts of adults and children, and spread to blood, lungs, middle ear or even the nervous system.[1] Infections caused by pneumococcus are currently a leading cause of invasive bacterial disease and a major cause of morbidity and mortality worldwide, especially among the elderly and young children,[2] and they are the main cause of bacterial pneumonia, usually of the lobar type, paranasal sinusitis and otitis media or meningitis, which is usually secondary to one of the former infections.[3,4] More than 90 different pneumococcal serotypes can be distinguished by their polysaccharide capsules, but approximately 90% of clinical episodes of invasive pneumococcal infections in humans are caused by 23 pneumococcal serotypes.[5] There is a limited efficacy of the available vaccines and the use of antibiotics results in either capsular type shifting or in the rapid appearance and spreading of antibiotic resistance determinants.[6,7]

The cell wall of *S. pneumoniae* is roughly six layers thick and is composed of peptidoglycan polymeric chains with teichoic acid substituents attached to approximately every third *N*-acetylmuramic acid.[1] Lipoteichoic acid is chemically identical to teichoic acid but it is attached to the cell membrane by a lipidic moiety. Both teichoic and lipoteichoic acids contain phosphorylcholine; two choline residues may be covalently bound to each pentasaccharide repeating unit. This is an essential element in the biology of *S. pneumoniae* since choline specifically adheres to choline-binding receptors that are located on virtually all human cells.[8] Besides, they are also recognized by host response components, such as the human C-reactive protein (CRP)[9] and the receptor of the platelet-activating factor (PAF).[10]

Keywords: Pce; Choline-binding protein; Homology modelling; Binuclear zinc centre; Ab initio calculations.
* Corresponding author. Tel.: +34 91 5622900; fax: +34 91 5644853; e-mail: nuria@suricata.iqm.csic.es
† These authors have contributed equally to this work.

0968-0896/$ - see front matter © 2005 Elsevier Ltd. All rights reserved.
doi:10.1016/j.bmc.2005.06.060

On the basis of functional genomic analysis, it is estimated that pneumococcus contains more than 500 surface proteins. Some of them are membrane-associated lipoproteins, while others are physically associated with the cell wall. The latter includes five penicillin-binding proteins[11] (PBPs), two neuraminidases[12] and an IgA protease.[13] A unique group of proteins on the pneumococcal surface is the family of choline-binding proteins (CBPs).[1,14,15] *S. pneumoniae* codes for four murein hydrolases, Lyt A,[16] Lyt B,[17] Lyt C[18] and phosphorylcholine esterase (Pce).[19–21] All CBPs share an N- or C-terminal module that is made up of homologous repeats of about 20 amino acids, while the additional module/s accounting for their specific functions are different. The choline-binding module (CBM) recognizes choline residues that are present in teichoic acids, allowing an attachment of the enzyme to the bacterial surface. Lyt A, Lyt B and Lyt C constitute the enzymatic machinery that is necessary for cell wall degradation, whereas Pce, a phosphorylcholine esterase, is involved in remodelling the distribution of choline residues that regulate the activity of other autolysins on the bacterial envelope by hydrolysing the phosphorylcholine residues from teichoic and lipoteichoic acid.[22]

Pce comprises a catalytic module located at the N-terminal part of the molecules and a C-terminal choline-binding module made up of 10 homologous repeating units, which are similar to sequence repeats present in other CBPs. It would be of great interest to gain additional information about Pce and the biological role of choline during infection by this pathogen as a potential way for developing new treatments of pneumococcal diseases. To this end, it is crucial to define the molecular structure and mechanism of this enzyme. On the basis of sequence similarity, the catalytic domain of Pce has been included into the metallo-β-lactamase fold family (PF00753) that comprises, among other enzymes, metallo-β-lactamases, glyoxalases, thiolesterases and phosphodiesterases.[23–27] The enzymes from this family usually bind two zinc ions per molecule as cofactor, and the presence of just one or both metal ions appears to be required for full catalytic activity.[25]

To gain insights that will increase our knowledge of Pce, not only from a structural point of view, but also concerning the role of Zn ions in the catalytic mechanism, we report herein a discussion of two possible tridimensional models of Pce. In addition, the potential ligands for the zinc binuclear cluster are proposed.

2. Materials and methods

2.1. Computational methods

2.1.1. Selection of templates. The identification of homologues of Pce (Swissprot code Q9AJT3) was carried out by performing sequence database searches with standard tools, such as PSI-BLAST[28], scanning the non-redundant protein sequence database at NCBI with an *E*-value cut-off of 10^{-4} and retaining only those matches with the most significant *E*-values. Besides, protein-fold recognition methods were applied using FUGUE,[29] a program for recognizing distant homologues by sequence structure comparison and 3D-PSSM.[30]

2.1.2. Alignment and adjustment. The most significant step of a homology model process is to obtain the correct sequence alignment of the target sequence with the homologues. Thus, this reliable sequence-structure mapping has allowed us to identify important structural features of the residues. The structure-based alignments for the found homologues were generated with COMPARER.[31,32] The target sequence Pce was added using the profile alignment facility of CLUSTALW,[33] followed by a manual adjustment of the multiple alignment sequence with the SEAVIEW[34] program guided by Pce secondary structure prediction with JPRED.[35] The alignment was annotated with JOY.[36]

2.1.3. Comparative modelling. We adopted a recursive approach comprising sequence alignment and model building. From the best alignment of template structures to the target sequence, 3D models containing all non-hydrogen atoms were automatically obtained using the method implemented in MODELLER (version 4.0).[37] The program deduces distance and angle constraints from a template structure and combines them with energy terms for adequate stereochemistry in an objective function that is later optimized in Cartesian space with conjugate gradients and molecular dynamic (simulated annealing) methods. Fifteen models of Pce were generated, but only the one with fewest restraints' violation and lowest energy was evaluated. Several cycles of realignment and model building were repeated until no further optimization of the model could be obtained.

The final model was evaluated with PROCHECK[38] and VERIFY3D.[39] JOY and COMPARER programs were used to generate structure-based alignments between the target and the template in every cycle of the model building process.

2.1.4. Docking of Zn ions into the active site. In the present study, the Zn atoms were placed according to the atomic coordinates of Zn–O–Zn system of the corresponding template. The Zn-coordinate systems were moved onto a Pce model using the option Fit Monomer of Sybyl.[40] Sybyl has not been completely parameterized for Zn ion, the atomic parameters of Zn ion being assigned according to Sybyl parameters.

Conformational search using Genetic Algorithm (GA) implemented in Sybyl package was performed to study the binding site of the Pce model. This program uses Genetic Algorithm, inspired by natural selection in evolution, as a global optimizer to locate the energy minima of molecules. Judson and Haydon[41] among other authors have shown that GAs provide a good, if not better, performance than other methods of conformational search. They scale well, making them suitable for large molecules. Several runs were carried out with a population size of 100 individuals, a set of constraints being used. Only the side chains of residues involved in the

active site were considered in this conformational search. During conformational search, distance restraints were also applied to the Zn–O distance. After examination of the docking model, structures were selected for further analyses using LPC[42] to generate protein–Zn ion interaction data.

2.1.5. Theoretical calculations. Ab initio and functional density theory (DFT) calculations on a simplified model of the active site have been carried out where Asp and His residues were replaced by CH_3COO^- and NH_3 molecules, respectively. This simplified model has been tested in the active site of a phosphodiesterase and thus, with this approach, optimized geometric parameter involving zinc ions did not show any significant changes.[43]

The ab initio molecular orbital and functional density theory (DFT) calculations were performed using the Gaussian 98 package.[44] The standard 6-31G* basis set at the Hartree–Fock level[45,46] (HF) and with the density functional calculation (DFT), B3LYP functional[47,48], were used. All structures were fully optimized without any symmetry restrictions in gas phase, until default convergence criteria of the program were satisfied.

2.2. Protein purification and site-directed mutagenesis

Pce phosphorylcholine esterase[21] was purified, from the cell extracts of *E. coli* BL21 (DE3) (pRGR12), by affinity chromatography on DEAE cellulose equilibrated with phosphate/Zn buffer (20 mM phosphate, 3 μM ZnCO3, pH 7.0), following a general procedure described elsewhere.[49] The protein was specifically eluted using a linear gradient (0–70 mM choline in 2 h; elution rate 1 ml/min) in phosphate/Zn buffer with 0.05 M NaCl. Homogeneity of protein preparations was confirmed by SDS-PAGE. Before use, protein solutions were extensively dialyzed against Hepes/Zn buffer (20 mM Hepes, 3 μM Zn^{2+}; $I = 0.05$, pH 7.0) and protein concentration was determined spectrophotometrically using a molar absorption coefficient of 194,020 M^{-1} cm^{-1} at 280 nm.

Pce H90A and D158A mutants were constructed by PCR site-directed mutagenesis.[50] According to this protocol, we used oligonucleotides complementary to the ends of the mature Pce encoding gene primer LytDN2 (5′-CCGAATTCAAGGAGATTAACATATGCAAGA AAGTTCAGGAAATAAAAT-3′, where EcoRI restriction site is underlined) and primer LytD-C (5′-TTGGA TCCCTACTACTGTTCTGATTCCGATTTG-3′, where BamHI restriction site is underlined) for the 5′ and 3′ ends, respectively, and two complementary oligonucleotides for each mutation: primer PceHA5′ (5′-CCACAG TGATGCTATTGGAAATGTT-3′) and primer PceH A3′ (5′-AACATTTCCAATAGCATCACTGTGG-3′) for H90A mutant and primer PceDA5′ (5′-CAGTTT GGGGCCATGGATATT-3′) and primer PceDA3′ (5′-AATATCCATGGCCCCAAACTG-3′) for D158A mutant. All these PCR-amplified fragments were cloned into plasmid pT7-7 and the DNA sequences of the mutants were confirmed by the dideoxy chain-termination method with an automated Abi Prism 3700™ DNA sequencer (Applied Biosystems). The recombinant strain cultures were expressed, using 50 μM isopropyl-thio-β-D-galactopyranoside as inducer, in *E. coli* BL21 (DE3) strain, and purified as wild-type Pce. All primers were synthesized on a Beckman model Oligo 1000M synthesizer. Restriction enzymes and other DNA modifying enzymes were purchased from Amersham.

2.2.1. Activity assays. Pce activity was assayed at 25 °C in Hepes/Zn^{2+} buffer using NPPC (*p*-nitrophenylphosphorycholine) as substrate by measuring the absorbance of the product, *p*-nitrophenol, at 410 nm.[21] Pce activity almost disappeared on extensive dialysis against Hepes buffer supplemented with 2 mM EDTA but was restored upon appropriate dilution into zinc-containing buffers.

3. Results and discussion

3.1. Comparative modelling

Because of its recent isolation, there is little information about Pce phosphorycholine esterase and its 3D structure has not yet been elucidated. To understand the binding characteristics of a Pce protein at the molecular level, we first conducted homology modelling studies. The PSI-Blast search for the catalytic domain of Pce did not give any close homologues as possible templates. Therefore, protein-fold recognition methods were applied (Table 1).

All templates show a metallo-β-lactamase fold and include three Zn-metallo-β-lactamases,[51–53] the human glyoxalase II[54]and the oxygen oxydoreductase (ROO) from *Desulfovibrio gigas,*[55] a Fe-containing enzyme. The metallo-β-lactamase L1 (code pdb 1sml),[51] secreted by pathogenic *Stenotrophomonas maltophilia*, and the human glyoxalase II (code pdb 1qh5)[54] provided the best ranking scores. The active sites of both enzymes contain a binuclear zinc-binding site, essential for full enzymatic activity, although they have different modes of zinc coordination.

Table 1. Ranking of fold using FUGUE and 3D-PSSM

Fold	Protein activity	From	PDB code	FUGUE score	3D-PSSM
Metallo-hydrolase	Zn metallo-β lactamase	*Stenotrophomonas maltophilia*	1sml	9.99	4.20 e^{-3}
Metallo-hydrolase	Glyoxalase II	*Human*	1qh5	7.96	3.75 e^{-4}
Flavodoxin-like	Oxygen oxydoreductase	*Desulfovibrio gigas*	1e5d	5.30	2.11 e^{0}
Metallo-hydrolase	Zn metallo-β lactamase	*Bacteroides fragilis*	1a7t	—[a]	3.08 e^{-2}
Metallo-hydrolase	Zn metallo-β lactamase	*Fluoribacter Gormanii*	1jt1	—[a]	3.42 e^{-2}

[a] FUGUE does not recognize it as distant homologue.

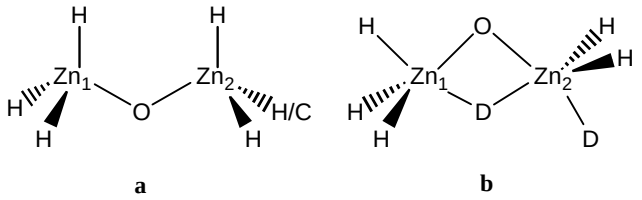

Figure 1. Coordination models of metallo-hydrolases of the metallo-β-lactamase fold: (a) coordination of metallo-β-lactamases and (b) coordination of human glyoxalase II.

The three metallo-β-lactamases show two closely spaced zinc ions that bind six protein residues with tetrahedral (Zn1) and distorted trigonal bipyramidal (Zn2) coordination,[51] and both ions are bridged by a water molecule (coordination A, Fig. 1a). In contrast, the two zinc ions of glyoxalase II,[54] coordinated by seven protein residues, show an octahedral coordination and are double bridged by an aspartic acid and a water molecule (coordination B, Fig. 1b).

A comparison of the structural alignment of predicted folds with the Pce sequence is shown in Figure 2 where the Zn-binding residues have been identified. There are some significant insertions but some of the key regions, such as those containing residues involved in zinc binding, are well-conserved. Besides, a number of residues involved in the right orientation of Zn- binding residues are also conserved. With regard to zinc donors, His 85, His 87, Asp 89, His 90 and His 228 (numbering from Pce sequence) are well-conserved among the sequences. Some structures, such as 1aj7t, show a cysteine instead of His 90 (numbering from Pce sequence). Asp 158 and Asp 203 (numbering of Pce) are not fully conserved (Fig. 2), with the latter involved in metal binding usually associated to coordination B.[25]

3.2. Model based on 1sml structure (Pce_1)

Considering the best-obtained ranking, a model using coordination A as pattern of coordination of Zn ions for Pce sequence was developed. Thus, we chose 1sml and 1a7t as representative members of Zn-metalloβ-lactamases to use them as templates for homology modelling. Three models of Pce were built based on found homologues according to the final alignment (Fig. 2a). Model 1a was based on 1sml structure with 14.5% of identity, model 1b was based on 1a7t structure with 12.6% of identity and model 1c was built using both structures as template. The three final models were analyzed on the basis of the values of the Ramachandran plot and of Verify 3D. The model 1a (Pce_1) showed the best validation values. Procheck summary of model Pce_1 showed that 87.9% of the residues were in the allowed region and only 2.4% in the disallowed region. The average score obtained with Verify 3D was 0.7, comparable to the value of 1sml (0.8). A comparison of the protein topologies is shown in Figure 3. The topographical diagrams show that secondary structure elements exhibit an αββα fold in all members of the metallo-β-lactamase family fold, whilst the Pce_1 model, having six α-helices (A–F) and eleven β-strands (1–11) (Fig. 3c), shows one more layer in the sandwich fold.

Taking into account the alignment shown in Figure 2, the residues involved in the coordination of the zinc would be His 85, His 87, Asp 89, His 90, Asp 158 and His 228. Residues His 85 and His 87 are located between β4 and helix B, while Asp 89 and His 90 participate in the formation of helix B. Of the other two residues, Asp 158 is located in a loop between β8 and β9, and His 228 is located just at the beginning of the loop following β11 (Fig. 3c).

3.3. Docking of Zn ion into the active site

Docking studies were carried out to investigate the metallic centre of Pce_1 model. An initial model of the metallic centre was obtained by transference of Zn–water–Zn system coordinates from 1sml structure to Pce_1. Then, a conformational search of the residues involved in the binding of Zn ions was carried out using GA. The 3D structure of a Zn-binding model for Pce_1 is shown in Figure 4 and the distances of Zn residues of the final model for Pce_1 are shown in Table 2. Most of the distances are within the range of experimental data in the templates, except for Asp 158 and Asp 89.

Taking into account the conservation of the Zn-binding residues among members of the metallo-β-lactamase fold family (Fig. 2a) and the resulting distances of Zn ions to the putative metal-binding residues, there are two doubtful residues: His 90 and Asp 158. Both of them are not fully conserved among the different enzymes and the distance of Asp 158 to Zn1 ion seems to be rather long. To establish the role of both these residues clearly, mutagenesis studies were carried out.

3.4. Mutational study

Enzyme kinetics and activities of the two mutants (H90A and D158A) of Pce were measured and compared with those of the wild-type enzyme (Table 3). The D158A mutant did not show a significant change in the catalytic constant, k_{cat}, although catalytic efficiency (k_{cat}/K_m) somewhat worsened. These results suggest that Asp 158 is not involved in the binding of zinc atoms. In contrast, mutation H90A decreases the activity to 12% of wild-type Pce and the catalytic efficiency by two orders of magnitude, proving that His 90 is actually involved in zinc coordination.

3.5. Model based on 1qh5 structure(Pce_2)

Disagreement between mutagenesis studies and theoretical model of coordination of Zn1 ion (Pce_1) could have arisen either due to a misalignment or/and a wrong coordination of Zn1 ion. The experimental data available suggest that both factors are likely contributing to this disagreement. The model was, therefore, reconstructed modifying both facts: the type of Zn-coordination and the alignment. In this sense, the Pce catalytic module was remodelled using as a representative template of the type of coordination B (Fig. 1b) the

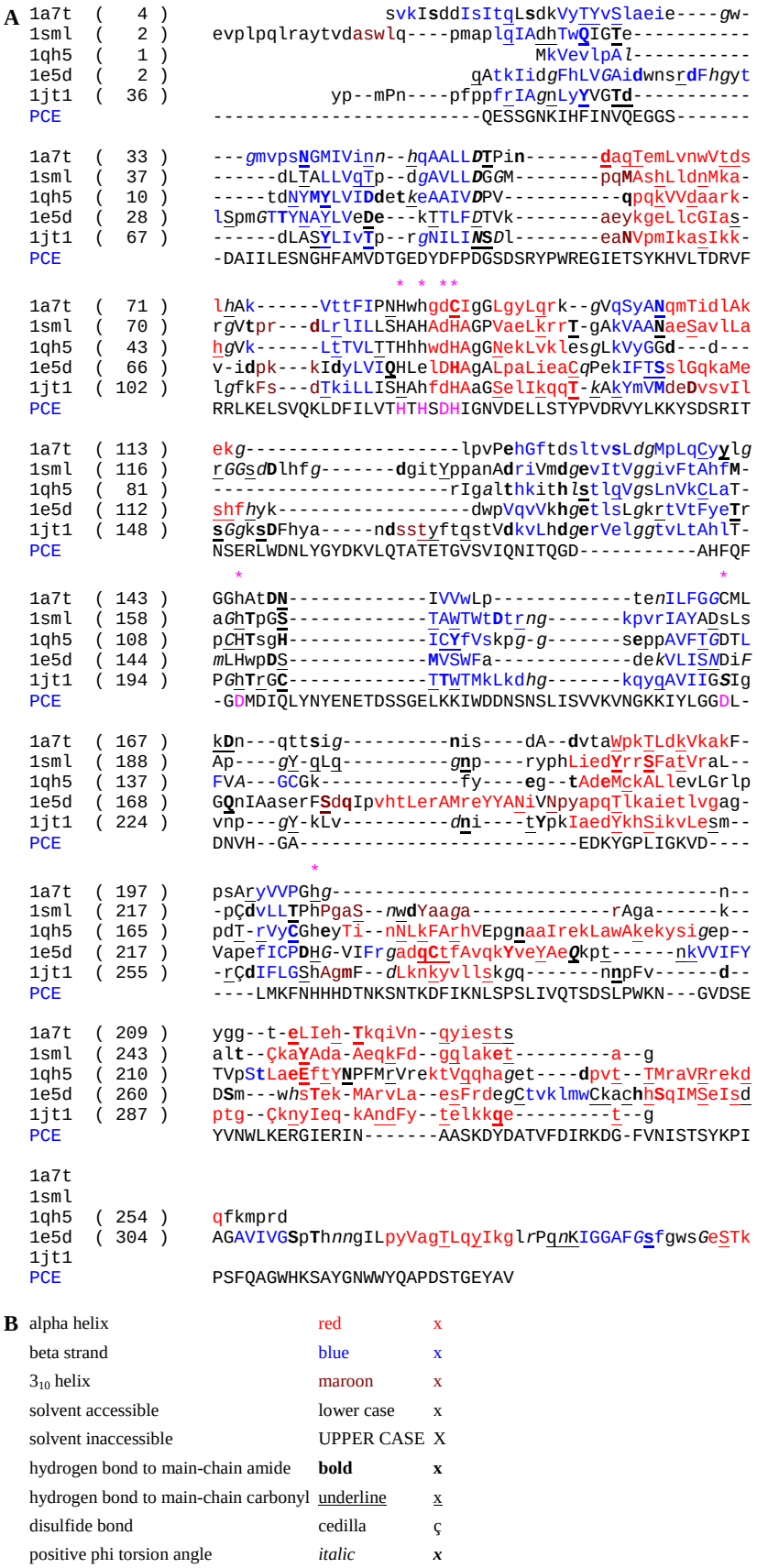

Figure 2. (A) Sequence alignment of predicted folds with Pce sequence generated by JOY. Asterisks (*) indicate the residues involved in the binding of the zinc atoms in a PCE1 model. (B) Key alignment of JOY.

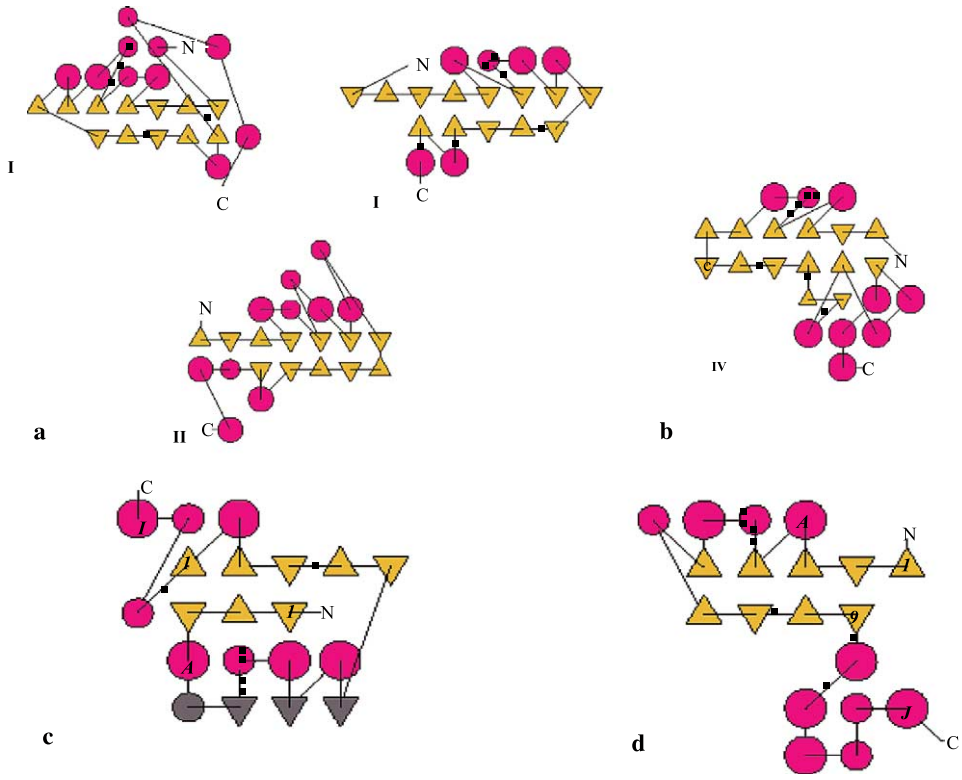

Figure 3. Topographical diagram of the arrangement of secondary structure elements of (a) metallo-β-lactamases (1sml (I), 1a7t (II) and 1jt1 (III)), (b) glyoxalase II (1qh5 (IV), C-terminal domain is included), (c) Pce_1 model and (d) Pce_2 model. Triangles represent β-strands and circles represent α-helices, the N- and C-termini being marked. The first and last helices and β-strands of Pce_1 (c) and Pce_2 (d) are indicated with letter (helices) and with number (β-strands). The positions of residues involved in the cofactor binding in Pce_1 and Pce_2 models are pointed out with black dots.

structure of human glyoxalase II (1qh5) and the alignment of the region comprising Asp 158 was modified (Fig. 5). The final model, Pce_2, was analyzed using values of the Ramachandran plot and Verify 3D. Procheck summary of Pce_2 showed that 86.1% of the residues were in the allowed region and only 4.0% in the disallowed region. The average score obtained with Verify 3D was 0.6 comparable to 0.7 of 1qh5 structure. The tertiary structure of Pce_2 shows the αββα folding motif characteristic of the metallo-β-lactamase family, with 10 α-helices (A–J) and nine β-strands (1-9) (Fig. 3d).

In accordance with the alignment shown in Figure 5, the residues involved in the coordination of the Zn atoms are His 85, His 87, Asp 89, His 90, Asp 171, Asp 203 and His 228. The transference of the Zn–water–Zn system coordinates from 1qh5 structure to Pce_2 model was carried out, followed by a conformational search of the residues involved in metal binding. The final 3D model for Pce_2 bimetallic cluster is shown in Figure 6. The distances of the residues to Zn ions of the final model (Table 2) are within the range of experimental data in 1qh5, except for Asp 171.

3.6. Ab initio calculation

The results obtained from Conformational Search using Genetic Algorithm (GA) implemented in Sybyl package are not completely in agreement with the experimental data of X-ray geometries, in particular the theoretical distances Asp–Zn are longer, especially the distance of Asp171–Zn in Pce_2 (Table 2).

Disagreement between the geometrical experimental data and theoretical model of penta-coordination of Zn ions in Pce_2 could be due to a wrong coordination of Zn ion in the model or due to the method of calculations used. Thus, with the two models (Pce_1 and Pce_2) on hand we decided to study the stability of both coordination modes of Zn ions by means of ab initio and DFT calculations on a simplified model of each active site of Pce_1 and Pce_2 to clarify the coordination environment of the zinc ions. The study in gas phase was performed using a molecular orbital ab initio method at the Hartree–Fock level with the 6-31G* basis set and a density functional theory (DFT), B3LYP/6-31G*. The results from the ab initio and DFT calculations are similar, indicating that both proposed simplified coordination models correspond to energy minima and that the geometries of these minimalist models are fairly in good agreement with the experimental data of X-ray geometries. In fact, both quantum models of the environment of Zn ions (Table 2) are compatible with the geometries of coordination models A (Pce_1) and B (Pce_2) obtained with GA calculations, indicating that in the simplified model Pce_2, coordination of the residue Asp171 with the Zn ion is possible.

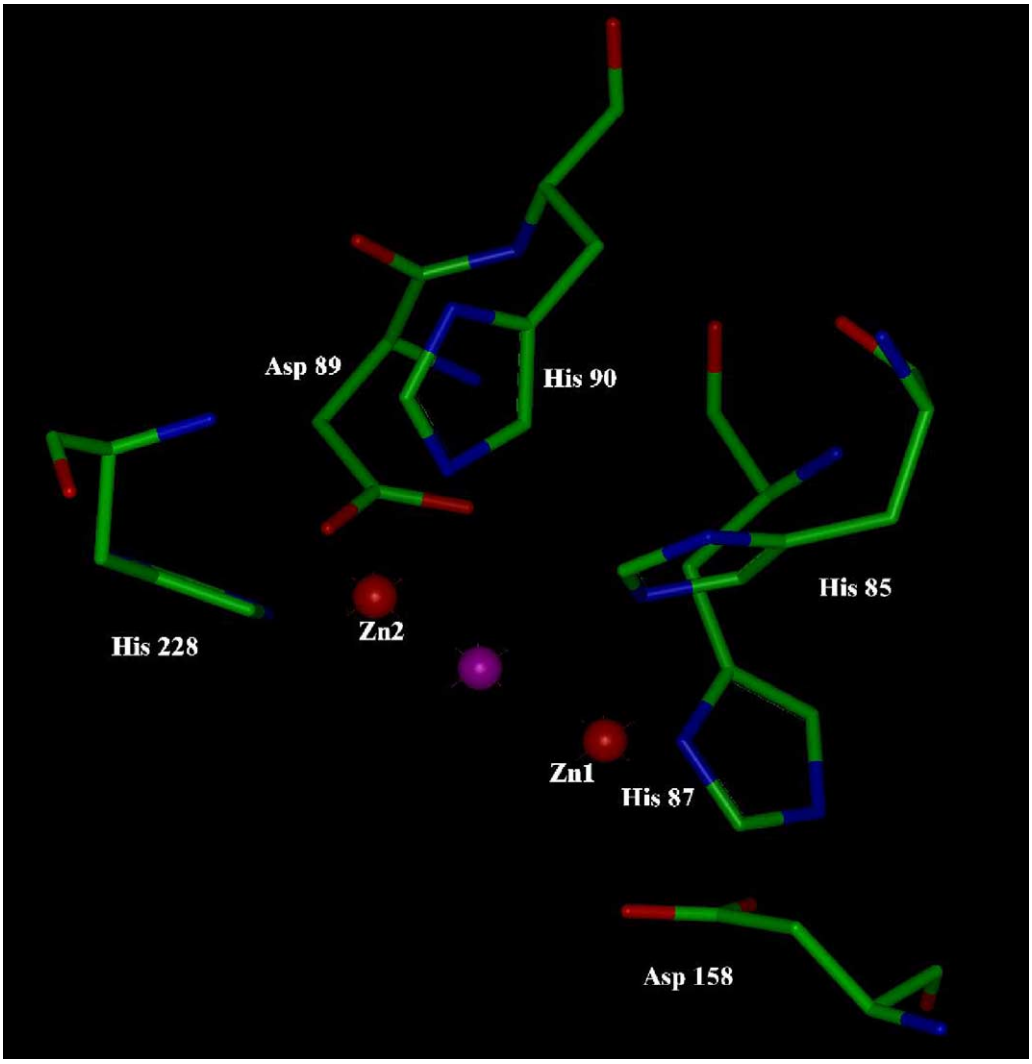

Figure 4. Three-dimensional structural model of the bimetallic zinc cluster of Pce_1. Only residues potentially involved in the cofactor binding are displayed in stick representation. Zinc ions are shown as red spheres, water as a magenta sphere, respectively. Hydrogens are omitted for clarity. The figure was generated using InsightII program.[57]

Table 2. Distances (Å) of the residues (aa) involved in the coordination of Zn atoms of X-ray structures (1sml and 1qh5) and both models of Pce (Pce_1 and Pce_2)

Structure	*d* Zn1–aa1	*d* Zn1–aa2	*d* Zn1–aa3	*d* Zn1–aa4	*d* Zn2–aa4	*d* Zn2–aa1	*d* Zn2–aa2	*d* Zn2–aa3	*d* Zn1–O–Zn2
	His84	His 86	His 160			Asp 88	His 89	His 225	
1SML	2.03	2.12	2.04	—	—	2.07	2.02	2.07	2.06, 1.87
	His85	His 87	Asp 158			Asp 89	His 90	His 228	
Pce_1[a]	2.29	1.66	3.30	—	—	3.26	2.02	1.94	2.24, 2.10
Pce_1(HF/6-31G*)[b]	2.12	2.11	1.97			1.99	2.13	2.12	1.94, 1.96
Pce_1(B3LYP/6-31G*)[c]	2.07	2.06	1.97			2.07	1.95	2.04	1.91, 1.95
	His 54	His 56	His 110	Asp 134	Asp 134	His 54	Asp 59	His 173	
1QH5	2.15	2.21	2.12	2.57	2.08	2.09	2.28	2.13	2.15, 2.02
	His85	His 87	Asp 171	Asp 203	Asp 203	Asp 89	His 90	His 228	
Pce_2[a]	2.32	2.32	4.82	1.61	3.24	3.05	2.55	1.66	2.15, 2.02
Pce_2(HF/6-31G*)[b]	2.29	2.16	1.98	2.13	2.28	2.03	2.13	2.12	1.95, 1.96
Pce_2(B3LYP/6-31G*)[c]	2.24	2.09	1.99	2.11	2.38	2.01	2.05	2.05	1.93, 1.95

[a] Distances of Pce models from conformational search using GA.
[b] Distances of simplified models from HF/6-31G* calculation.
[c] Distances of simplified models from B3LYP/6-31G* calculation.

Table 3. Hydrolytic activity of *S. pneumoniae* wild-type Pce and the H90A and D158A mutants on NPPC[a]

	K_m (mM)	k_{cat} (s^{-1})	k_{cat}/K_m ($mM^{-1}\ s^{-1}$)
Wild type	0.16 ± 0.02	9.3 ± 0.2	58 ± 6
H90A	1.7 ± 0.4	1.13 ± 0.07	0.7 ± 0.1
D158A	0.47 ± 0.06	7.1 ± 0.2	15 ± 2

[a] Measurements were made in Hepes/Zn buffer at 25 °C ($I = 0.05$).

4. Conclusions

To summarize, two spatial models of the catalytic module of pneumococcal phosphorylcholine esterase (Pce) are described. These models are based on templates belonging to hydrolases of the metallo-β-lactamase fold family (1sml, 1a7t, 1jt1 and 1qh5) displaying two different coordination modes of the zinc ions acting as cofactor. The drastic drop in Pce activity observed upon dialysis against EDTA-containing buffer and its recovery upon addition of Zn salts (see Materials and methods) show that Pce is a zinc-dependent phosphorylcholine esterase. Docking studies with zinc ions were employed to find out the residues involved in coordination of the metallic cofactor and to understand the role of particular residues in metal binding.

The first model (Pce_1) was built by homology modelling of the 1sml structure. The fact that the mutant generated by substitution of His 90, a ligand of Zn2, by alanine showed a highly reduced activity supports its implication in Zn coordination and the existence of two Zn atoms in the catalytic centre. However, the Pce_1 model fails in the prediction of Asp 158 participating in the binding of Zn1.

The second model (Pce_2) obtained by homology modelling from 1qh5 shows a binuclear Zn-binding site, according to the mutational study. Both zinc ions show a penta-coordination and they would be bridged, as in human glyoxalase II, *Desulfovibrio gigas* oxygen oxidoreductase and other metallo-hydrolases containing binuclear zinc cocatalytic centres,[56] by a water molecule and Asp 203. The Pce_2 model shows a fold similar to those of metallo-β-lactamase family members and the spatial distribution of residues involved in the binding of zinc ions is consistent with the experimental data.

The relevance of His 90 in Pce activity suggests that both metal ions are directly involved in the catalytic process and support the presence of a binuclear zinc cocatalytic centre in the active site of Pce. Double bridging of zinc atoms by a solvent molecule and an aspartic or glutamic acid is a characteristic feature of cocatalytic centres in zinc metallo-hydrolases[61] and would be consistent with the coordination type proposed in a Pce_2 model. In contrast, the coordination in a Pce_1 model seems to be found in systems, such as β-lactamases, whose

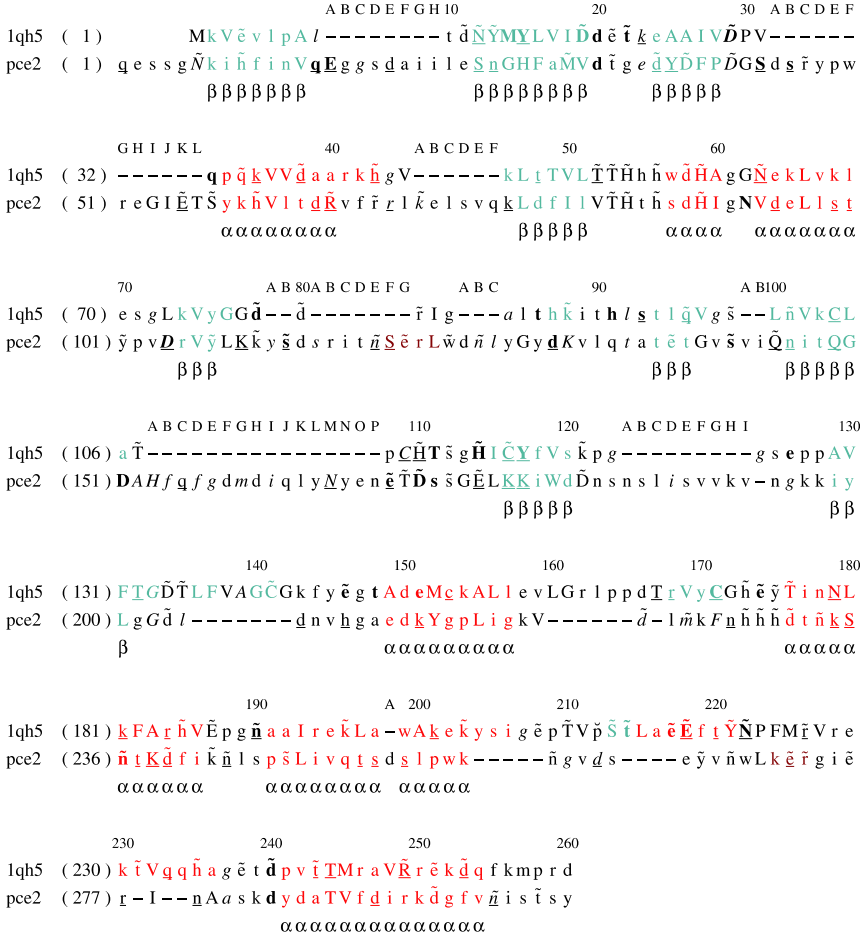

Figure 5. JOY output of the structural superposition of the template 1qh5 and Pce_2, model.

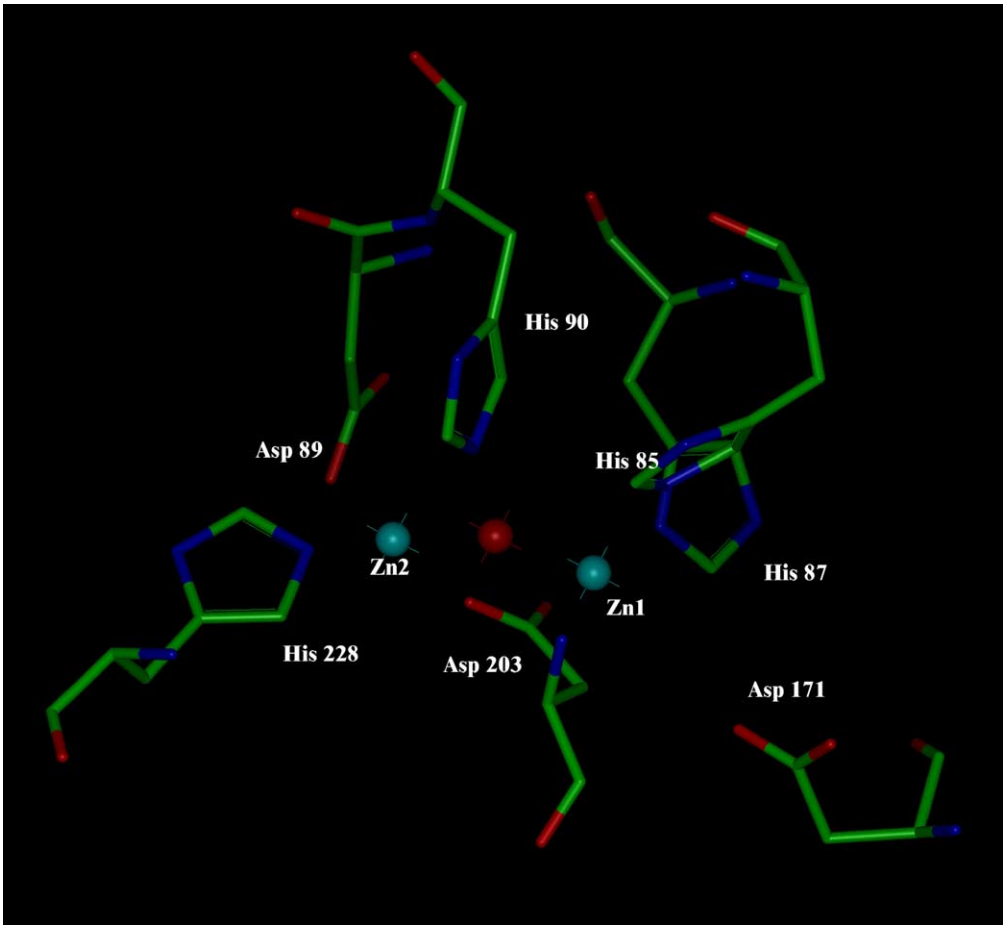

Figure 6. Three-dimensional structural model of the bimetallic zinc cluster of Pce_2. Only residues potentially involved in the cofactor binding are displayed in stick representation. Zinc ions are shown as blue spheres, water as a red sphere, respectively. Hydrogens are omitted for clarity. The figure was generated using InsightII program.[57]

activity depends on the presence of a first zinc ion (Zn1), while binding of a second metal equivalent (Zn2) may have different effects on activity.[23] Since the pneumococcal phosphorylcholine esterase is an interesting therapeutic target, these studies contribute to imparting knowledge of a Pce catalytic mechanism.

References and notes

1. López, R.; García, E. *FEMS Microbiol. Rev.* **2004**, *28*, 553–580.
2. Binder, S.; Levitt, A. M.; Sacks, J. J.; Hughes, J. M. *Science* **1999**, *284*, 1311–1313.
3. Hirst, R. A.; Kadioglu, A.; Oćallaghan, C.; Andrew, P. W. *Clin. Exp. Immunol.* **2004**, *138*, 195–201.
4. Casal, J.; Tarrago, D. *Curr. Opin. Infect. Dis.* **2003**, *16*, 219–224.
5. Neralla, S.; Meyer, K. C. *Drugs Aging* **2004**, *21*, 851–864.
6. Dagan, R. *Curr. Opin. Otolaryngol. Head Neck Surg.* **2004**, *12*, 488–494.
7. McCormick, A. W.; Withney, C. G.; Farley, M. M.; Lynfield, R.; Harrison, L. H.; Bennett, N. M.; Schaffner, W.; Reingold, A.; Hadler, J.; Cieslak, P.; Samore, M. H.; Lipsitch, M. *Nat. Med.* **2003**, *9*, 424–430.
8. Bozdogan, B.; Bogdanovich, T.; Kosowska, K.; Jacobs, M. R.; Appelbaum, P. C. *Curr. Drug Targets Infect. Disord.* **2004**, *4*, 169–176.
9. Hirschfield, G. M.; Pepys, M. B. *QJM* **2003**, *96*, 793–807.
10. Cundell, D. R.; Weiser, J. N.; Shen, J.; Young, A.; Tuomanen, E. I. *Infect. Immun.* **1995**, *63*, 757–761.
11. Popham, D. L.; Young, K. D. *Curr. Opin. Microbiol.* **2003**, *6*, 594–599.
12. Achyuthan, K. E.; Achyuthan, A. M. *Comp. Biochem. Physiol. B Biochem. Mol. Biol.* **2001**, *129*, 29–64.
13. Parsons, H. K.; Vitovski, S.; Sayers, J. R. *Biochem. Soc. Trans.* **2004**, *32*, 1130–1132.
14. López, R.; García, E.; García, P.; García, J. L. *Microb. Drug Resist.* **1997**, *3*, 199–211.
15. Rosenow, C.; Ryan, P.; Weiser, J. N.; Johnson, S.; Fontan, P.; Ortqvist, A.; Masure, H. R. *Mol. Microbiol.* **1997**, *25*, 819–829.
16. García, E.; García, J. L.; Ronda, C.; García, P.; López, R. *Mol. Gen. Genet.* **1985**, *201*, 225–230.
17. García, P.; González, M. P.; García, E.; López, R.; García, J. L. *Mol. Microbiol.* **1999**, *31*, 1275–1277.
18. García, P.; González, M. P.; García, E.; López, R.; García, J. L. *Mol. Microbiol.* **1999**, *33*, 128–138.
19. García, J. L.; Díaz, E.; Romero, A.; García, P. *J. Bacteriol.* **1994**, *176*, 4066–4072.
20. Tomasz, A.; Moreillon, P.; Pozzi, G. *J. Bacteriol.* **1988**, *170*, 5931–5934.
21. De las Rivas, B.; García, J. L.; López, R.; García, P. *Microb. Drug Resist.* **2001**, *7*, 213–222.
22. Vollmer, W.; Tomasz, A. *Mol. Microbiol.* **2001**, *39*, 1610–1622.

23. Helfand, M. S.; Bonomo, R. A. *Curr. Drug Targets Infect. Disord.* **2003**, *3*, 9–23.
24. Bonfiglio, G.; Russo, G.; Nicoletti, G. *Expert Opin. Investig. Drugs* **2002**, *11*, 529–544.
25. Rasia, R. M.; Ceol'in, M.; Vila, A. J. *Protein Sci.* **2003**, *12*, 1538–1546.
26. Bush, K. *Clin. Infect. Dis.* **2001**, *32*, 1085–1089.
27. Daiyasu, H.; Osaka, K.; Ishino, Y.; Toh, H. *FEBS Lett.* **2001**, *503*, 1–6.
28. Altschul, S. F.; Madden, T. L.; Schaffer, A. A.; Zhang, J.; Zhang, Z.; Miller, W.; Lipman, D. J. *Nucleic Acids Res.* **1997**, *1*, 3389–3402.
29. Shi, J.; Blundel, T. L.; Mizuguchi, K. *J. Mol. Biol.* **2001**, *310*, 243–257.
30. Kelley, L. A.; MacCallum, R. M.; Sternberg, M. E. *J. Mol. Biol.* **2000**, *299*, 499–520.
31. Sali, A.; Blundell, T. *J. Mol. Biol.* **1990**, *20*, 403–428.
32. Zhu, Z. Y.; Sali, A.; Blundell, T. *Protein Eng.* **1992**, *5*, 43–51.
33. Thompson, J. D.; Gibson, T. J.; Plewniak, F.; Jeanmougin, F.; Higgins, D. G. *Nucleic Acids Res.* **1997**, *25*, 4876–4882.
34. Galtier, N.; Gouy, M.; Gautier, C. *Comput. Appl. Biosci.* **1996**, *12*, 543–548.
35. Cuff, J. A.; Clamp, M. E.; Siddiqui, A. S.; Finlay, M.; Barton, G. J. *Bioinformatics* **1998**, *14*, 892–893.
36. Mizuguchi, K.; Deane, C.; Blundell, T.; Johnson, M. S.; Overington, J. P. J. *Bioinformatic* **1998**, *14*, 617–623.
37. Sali, A.; Blundell, T. *J. Mol. Biol.* **1993**, *234*, 779–815.
38. Luthy, R.; Bowie, J. U.; Eisenberg, D. *Nature* **1992**, *5*, 583–585.
39. Laskowski, R. A.; McArthur, W.; Moss, D.; Thornton, J. M. *J. Appl. Crystallogr.* **1993**, *26*, 283–291.
40. SYBYL 6.9, Tripos Inc., 1699 South Hanley Rd., St. Louis, MO 63144, USA.
41. Judson, O. P.; Haydon, D. *J. Mol. Evol.* **1999**, *49*, 539–550.
42. Sobolev, V.; Sorokine, A.; Prilusky, J. E.; Abola, E.; Edelman, M. *Bioinformatics* **1999**, *15*, 327–332.
43. Koca, J. V.; Zhan, C. G.; Rittenhouse, R. C.; Ornstein, R. L. *J. Comput. Chem.* **2003**, *24*, 368–378.
44. Frisch, M. J.; Trucks, G. W.; Schlegel, H. B.; Scuseria, G. E.; Robb, M. A.; Cheeseman, J. R.; Zakrzewski, V. G.; Montgomery, J. A.; Stratmann, R. E.; Burant, J. C.; Dapprich, S.; Millam, J. M.; Daniels, A. D.; Kudin, K. N.; Strain, M. C.; Farkas, O.; Tomasi, J.; Barone, V.; Cossi, M.; Cammi, R.; Mennucci, B.; Pomelli, C.; Adamo, C.; Clifford, S.; Ochterski, J.; Petersson, G.A.; Ayala, P. Y.; Cui, Q.; Morokuma, K.; Salvador, P.; Dannenberg, J. J.; Malick, D. K.; Rabuck, A. D.; Raghavachari, K.; Foresman, J. B.; Cioslowski, J.; Ortiz, J. V.; Baboul, A. G.; Stefanov, B. B.; Liu, G.; Liashenko, A.; Piskorz, P.; Komaromi, I.; Gomperts, R.; Martin, R.L.; Fox, D. J.; Keith, T.; Al-Laham, M. A.; Peng, C. Y.; Nanayakkara, A.; Challacombe, M.; Gill, P. M. W.; Johnson, B.; Chen, W.; Wong, M. W.; Andres, J. L.; Gonzalez, C.; Head-Gordon, M.; Replogle, E. S.; Pople, J. A. Gaussian, Inc., GAUSSIAN 98, Pittsburgh, PA, 2001.
45. Cramer, C. J.; Truhlar, D. G. *Chem. Rev.* **1999**, *99*, 2161–2200.
46. Francl, M. M.; Pietro, J.; Hehre, W. J.; Binkley, J. S.; Gordon, M. S.; De Frees, D. J.; Pople, J. A. *J. Chem. Phys.* **1982**, *77*, 3654–3665.
47. Becke, A. D. *J. Chem. Phys.* **1993**, *98*, 5648–5652.
48. Lee, C.; Yang, W.; Parr, R. G. *Phys. Rev. B.* **1988**, *37*, 785–789.
49. Sambrook, J.; Russell, D. W. *Molecular Cloning: A Laboratory Manual*, 3rd ed.; Cold Spring Harbor Laboratory Press: New York, 2001.
50. Sánchez-Puelles, J. M.; Sanz, J. M.; García, J. L. *Gene* **1990**, *89*, 69–75.
51. Ullah, J. H.; Walsh, T. R.; Taylor, I. A.; Emery, D. C.; Verma, C. S.; Gamblin, S. J.; Spencer, J. *J. Mol. Biol.* **1998**, *284*, 125–136.
52. Frazao, C.; Silva, G.; Gomes, C. M.; Matias, P.; Coelho, R.; Sieker, L.; Macedo, S.; Liu, M. Y.; Oliveira, S.; Teixeira, M.; Xavier, AV.; Rodrigues-Pousada, C.; Carrondo, M. A.; Le Gall, J. *Nat. Struct. Biol.* **2000**, *7*, 1041–1045.
53. Garc'ia-Saez, I.; Mercuri, P. S.; Papamicael, C.; Kahn, R.; Frere, J. M.; Galleni, M.; Rossolini, G. M.; Dideberg, O. *J. Mol. Biol.* **2003**, *325*, 560–651.
54. Cameron, A. D.; Ridderstrom, M.; Olin, B.; Mannervik, B. *Struct. Fold. Des.* **1999**, *7*, 1067–1078.
55. Fitzgerald, P. M.; Wu, J. K.; Toney, J. H. *Biochemistry* **1998**, *37*, 6791–6800.
56. Auld, D. S. *BioMetals* **2001**, *14*, 271–313.
57. InsightII. Biosym, San Diego, CA, USA.